Comparison of the Solution Conformation and Dynamics of Antifreeze Glycoproteins from Antarctic Fish

Andrew N. Lane,* Lisa M. Hays,† Nelly Tsvetkova,† Robert E. Feeney,‡ Lois M. Crowe,† and John H. Crowe†
*Division of Molecular Structure, National Institute for Medical Research, London NW7 1AA, United Kingdom, and †Section of Molecular and Cellular Biology and ‡Department of Food Science and Technology, University of California, Davis, California 95616 USA

ABSTRACT The ^{1}H- and ^{13}C-NMR spectra of antifreeze glycoprotein fractions 1–5 from Antarctic cod have been assigned, and the dynamics have been measured using ^{13}C relaxation at two temperatures. The chemical shifts and absence of non-sequential ^{1}H-^{1}H NOEs are inconsistent with a folded, compact structure. ^{13}C relaxation measurements show that the protein has no significant long-range order, and that the local correlation times are adequately described by a random coil model. Hydroxyl protons of the sugar residues were observed at low temperature, and the presence of exchange-mediated ROEs to the sugar indicate extensive hydration. The conformational properties of AFGP1–5 are compared with those of the previously examined 14-mer analog AFGP8, which contains proline residues in place of some alanine residues (Lane, A. N., L. M. Hays, R. E. Feeney, L. M. Crowe, and J. H. Crowe. 1998. *Protein Sci.* 7:1555–1563). The infrared (IR) spectra of AFGP8 and AFGP1–5 in the amide I region are quite different. The presence of a wide distribution of backbone torsion angles in AFGP1–5 leads to a rich spectrum of frequencies in the IR spectrum, as interconversion among conformational states is slow on the IR frequency time scale. However, these transitions are fast on the NMR chemical shift time scales. The restricted motions for AFGP8 may imply a narrower distribution of possible ø, ψ angles, as is observed in the IR spectrum. This has significance for attempts to quantify secondary structures of proteins by IR in the presence of extensive loops.

INTRODUCTION

To prevent the formation of large ice crystals in blood and tissue at low temperatures, many species, including polar fish and insects, manufacture high concentrations of proteins that inhibit the growth of ice crystals, lowering the freezing point, with only a small effect on the melting temperature. This non-colligative property is distinct from equilibrium freezing point depression, and can be observed as hysteresis in ice formation in cooling/warming cycles. This is possibly due to binding on one or more ice facet, preventing further growth (for a review, see Yeh and Feeney, 1996).

Several antifreeze proteins have been isolated and described, and they fall into four distinct structural classes (Davies and Sykes, 1997). All of these proteins form ordered, compact structures similar to other globular proteins. Although there are numerous theories of their action, there is little consensus as to the mechanism of ice binding of these diverse proteins. In Antarctic fish species, the blood and tissues contains high concentrations of a number of related antifreeze glycoproteins. These proteins are based on a repeated sequence of AAT*, where T* is threonine with the disaccharide Gal-1, 3GalNAc bonded to the Oβ of the threonine residue. The various fractions that have been described differ mainly in the number of repeats, though fraction 8 in particular is not only short (14–16 residues), but also contains some of the alanine residues substituted by proline. These short glycopeptides are the most abundant, but on a weight basis are less potent in preventing ice crystallization.

Recently we described the conformational preferences and local dynamics of AFGP8 (Lane et al., 1998). According to the NMR spectra, there was no significant long-range order, and substantial segmental flexibility. However, for the Thr-Pro-Ala tripeptides, evidence was obtained of some local order forming a small segment of secondary structure reminiscent of the polyproline helix (Lane et al., 1998). The high degree of flexibility of these peptides suggests that the mechanism of action may be fundamentally different from the non-glycosylated AFPs (Yeh and Feeney, 1996; Davies and Sykes, 1997; Harding et al., 1999; Haymet et al., 1999), as there is no fixed long-range structure present. To provide further information on the conformational preferences of these glycoproteins, we have investigated the solution properties of AFGP1–5, which contain no proline residues, and vary in length from 60 to 120 residues. We have assigned the ^{1}H- and ^{13}C-NMR spectra of AFGP1–5, and determined its dynamic properties by ^{13}C-NMR relaxation measurements at two temperatures. We have also used FTIR spectroscopy to provide further information about the local backbone conformation of both AFGP1–5 and AFGP8. The amide I region of the spectrum ($\sim$1600–1700 cm^{-1}) reports on the peptide carbonyl stretching frequency, which is sensitive to the local conformation (Byler and Susi, 1986; Dong et al., 1990; Pestrelski et al., 1991; Surewicz et al., 1993).

Received for publication 15 November 1999 and in final form 24 February 2000.

Address reprint requests to Andrew N. Lane, Division of Molecular Structure, National Institute for Medical Research, The Ridgeway, Mill Hill, London NW7 1AA, UK. Tel.: 44-208-959-3666; Fax: 44-208-906-4477; E-mail: alane@nimr.mrc.ac.uk.

Abbreviations used: AFP, antifreeze proteins; AFGP, antifreeze glycoproteins; DQFCOSY, double quantum filtered correlation spectroscopy; FTIR, Fourier transform infrared spectroscopy; HSQC, heteronuclear single quantum coherence; TOCSY, total correlation spectroscopy.

0006-3495/00/06/3195/13 $2.00

To reconcile the NMR and FTIR results, we invoke a dynamic model that incorporates the different time scales probed by these methods. In addition, results from MD calculations on short peptide sequences related to those present in AFGPs show that local backbone fluctuations of the appropriate magnitude do occur on the correct general time scale.

MATERIALS AND METHODS

Materials

AFGP1–5 was isolated from the Antarctic fish *Trematomus borchgrevinki* and purified as previously described (DeVries et al., 1970). This preparation contains five homologs of the repeating tripeptide AAT* that differ in the number of repeats *n*. AFGP3–5 account for >80% of the total, and vary from 11 to 22 kDa. (DeVries et al., 1970). Integration of signals in both ^{1}H and ^{13}C 1D-NMR spectra acquired with long relaxation delays showed that the relative concentrations of each sugar and amino acid residue were equal to within better than 10%.

For NMR analysis, the AFGP1–5 sample was dissolved in d_3-acetate buffer pD* = 5 at 17 mg/ml. For FTIR measurements, AFGP1–5 and AFGP8 were dissolved in 10 mM phosphate buffer pH 7.4 at 50 mg/ml.

PolyPro (1–10 kDa) was purchased from Sigma Chemical Co. (St. Louis, MO) and used without further purification. Aprotinin, hen egg white lysozyme, and bovine carbonic anhydrase were purchased from Sigma Chemical Co. (Poole, Dorset, UK). For NMR they were dissolved in a deuterated buffer containing 20 mM sodium phosphate and 100 mM KCl, pH 7.

The peptides NAcAATAA and NAcAAPAA were synthesized using fmoc chemistry on an Applied Biosystems 430A peptide synthesizer and purified by reverse-phase HPLC on a preparative C18 column using a 1% acetonitrile-water gradient. The composition and purity were verified by NMR spectroscopy.

Methods

NMR spectroscopy

^{13}C-NMR spectra were recorded in D_2O at 9.4 T on a Bruker AM400 as previously described (Lane et al., 1998). ^{1}H-NMR and ^{1}H-detected ^{13}C-NMR spectra were recorded at 14.1 T on a Varian Unity spectrometer and at 11.75 T on a Varian UnityPlus spectrometer. Spectra in H_2O were recorded using Watergate (Piotto et al., 1992) for solvent suppression. TOCSY spectra were recorded using MLEV-17 to provide the spin-lock (Bax and Davis, 1985).

^{13}C relaxation times were determined at 9.4 T at 303 K and 283 K by fast inversion recovery (T_1) (Gupta et al., 1980), FRESCO (T_2) (Forster, 1989), and the gated decoupling experiment (NOE). The relaxation delay for the NOE was 4 s (>5 times the longest T_1 value). R_1 and R_2 time courses were analyzed by nonlinear regression to a single exponential using peak heights as previously described (Lane et al., 1998). Relaxation data were obtained from at least two measurements at each temperature.

The relaxation rate constants were analyzed using the program Relaxm (A. N. Lane, unpublished data). This program searches exhaustively for the overall correlation time, the order parameter, and the internal correlation time for each site in the molecule within the framework of the formalism of Lipari and Szabo (1982) as described (Schurr et al., 1994; Alexandrovich et al., 1999; McIntosh et al., 2000):

$$R_1 = (\alpha/r^6)[J(\Delta\omega) + 3J(\omega_N) + 6J(\textstyle\sum\omega)] + 6\beta(\Delta\sigma)^2\omega_N^2 J(\omega_N) \quad (1)$$

$$R_2 = (\alpha/2r^6)[4J(0) + J(\Delta\omega) + 3J(\omega_N) + 6J(\omega_H) + 6J(\textstyle\sum\omega)] + \beta(\Delta\sigma)^2\omega_N^2[4J(0) + J(\omega_N)] + R_x \quad (2)$$

$$\mathrm{NOE} = 1 + (\gamma_H/\gamma_N)(\alpha/r^6)[6J(\textstyle\sum\omega) - J(\Delta\omega)]/R_1 \quad (3)$$

where α = 3.56 Å^6 ns^{-1}, β = 22.22 10^{-6}, $\Delta\sigma$ is the chemical shift anisotropy (CSA) in ppm (~25 ppm), r is the C–H bond length (1.095 Å) (Nicholson et al., 1996), and R_x is the exchange contribution to R_2.

For a spherical molecule with rapid internal motions, the spectral density functions are (Lipari and Szabo, 1982):

$$J(\omega) = S^2\tau_0/(1 + \omega^2\tau_0^2) + (1 - S^2)\tau_e/(1 + \omega^2\tau_e^2) \quad (4)$$

where τ_0 is the rotational correlation time of the molecules, τ_e is the effective correlation time for fast internal motion, and S^2 is the generalized order parameter. Calculations were carried out using just the NOE and R_1 values and with R_1, R_2, and NOE. For each C–H vector, the value of τ_0 was varied from 2 to 10 ns in steps of 0.04 ns, S^2 in steps of 0.02, and τ_e in steps of 5 ps, i.e., at least 20 million calculations at each temperature. We found that for some sites, quite poor fits were obtained unless R_x was non-zero. An estimate of R_x was obtained from the difference between the observed value of R_2, and that calculated from the value calculated from the best-fit τ_0 and S^2 found using the R_1 and NOE data only.

The translational diffusion coefficient was measured at 14.1 T in D_2O at 30°C and 10°C using the pulsed field gradient stimulated echo method (Tanner, 1970; Gibbs and Johnson, 1991). The sample was restricted to 16 mm along the z axis in a 5-mm Shigemi NMR tube. 1D spectra were acquired with two echo times as a function of gradient strength (32 linearly spaced values). The decay of the intensity was monitored by integrating regions of baseline-corrected spectra, or peak heights. The integrated intensity of several regions of the spectrum were fitted using nonlinear regression to the Gaussian decay function:

$$I = I_0\exp(-\gamma^2 G_Z^2 D\delta^2(t - \delta/3)) \quad (5)$$

where G_z is the z-gradient strength, D is the diffusion coefficient, γ is the gyromagnetic ratio, t is the gradient echo time, and δ is the length of the gradient pulse. The linearity of G_z was checked using Gd^{3+}-doped D_2O, and was found be acceptable using a 16 mm solution column in 5-mm Shigemi tubes. The B_1 field gradient over this length is essentially linear. HOD and test proteins were used to verify the accuracy of the gradient strengths. The diffusion coefficients were compared with those of the standard proteins aprotinin (M_r = 6500), hen egg white lysozyme (M_r = 14200), and carbonic anhydrase (M_r = 29,000), all recorded at 10 mg/ml.

Infrared spectroscopy

FTIR spectra were recorded on a Perkin-Elmer FTIR model 2000 spectrometer (Norwalk, CT), assisted by a microcomputer running Perkin-Elmer's Spectrum software. The sample compartment was flushed with dry air from a Whatman model 75-62 generator (Whatman Inc., Haverhill, MA), and the spectra were recorded at a relative humidity of 0%, and at room temperature (~23°C). Samples were introduced between CaF_2 windows separated with a 6-μm Mylar spacer. Single-beam spectra of buffer and sample were recorded in the same cell to guarantee a constant path length; 256 scans were co-added for each spectrum, with a resolution of 4 cm^{-1}. The difference between the sample and buffer spectra was calculated such that the region around 2100 cm^{-1} (corresponding to a water band) was flat. The spectrum of water vapor was recorded using an empty sample chamber exposed to ambient air. The water vapor spectrum was then subtracted from the sample spectrum with a weighting such that the second derivative spectrum in the region 1900–1700 cm^{-1} was flattened. The corrected spectrum was finally smoothed using a nine-point Savitzky-Golay function. This had very little effect on the spectrum owing to the

high signal-to-noise ratio of the original data. Comparable results were obtained whether smoothing was applied or not. The amide I region (1600–1700 cm^{-1}) of the spectrum was baseline-flattened using the Spectrum software. This routine produces a spline curve under the spectrum, which is then subtracted, producing a flat baseline. The resulting spectrum was then exported to Sigmaplot v 2.0 and Peak Fit v 4.0 (Jandel Scientific Corp, San Rafael, CA) for further analysis. The resolution-enhanced spectra were analyzed as a sum of Gaussian peaks having different bandwidths. The frequencies are diagnostic of structure type, and the relative peak areas provide an estimate of the relative concentrations of each structural type present. The entire fitting procedure was verified by comparing spectra of α-chymotrypsinogen with published values. We obtained results almost identical to those reported by Allison et al. (1996).

The method of Fourier self-deconvolution was also applied to the spectra to enhance the resolution, using the Fourier deconvolution routine in the Spectrum software. Reference spectra of protein standards were also acquired and processed in a similar way.

Because of the different degrees of resolution enhancement, the appearance of the spectra is not identical after these treatments. Nevertheless, peak fitting to the resolution-enhanced spectra (sum of Gaussian peak shapes) gives an estimate of the relative areas of each frequency band. These bands were then assigned on the basis of frequency to apparent secondary structure types (Byler and Susi, 1986; Dong et al., 1990; Pestrelski et al., 1991). We note that this does not mean that such structures are actually present in these samples, rather that there are sets of ø, ψ angles and that these are responsible for the different observed frequencies (see below).

MD calculations

Molecular dynamics simulations were run for AATAA and AAPAA both in vacuo and in a water bath at 300 K using either the CFF91 or Amber force fields using Discover98 (Molecular Simulations Inc., San Diego, CA). For the simulations in vacuo, a distance-dependent dielectric constant of $\epsilon = 4r$ was used. The peptide was generated as an extended chain, with an N-terminal ammonium and a C-terminal carboxylate group (corresponding to neutral pH), energy-minimized (100 steps of conjugate gradients), and followed by 1 ps equilibration free dynamics at 300 K. The system was then further allowed to evolve for 500 ps under the same conditions. For simulations in water, the same extended chain was energy minimized in a box of water molecules. In these calculations the dielectric constant was set to unity. The system was then equilibrated over 10 ps dynamics at 300 K, followed by 400 ps free dynamics. Coordinate files were stored every 100 fs. Torsion angles ø and ψ were analyzed using the graphing functions within InsightII (Molecular Simulations).

RESULTS

NMR assignments of AFGP1–5

Protons were assigned to spin type using DQF-COSY in D_2O (Fig. 1) and TOCSY (Fig. 2 *A*) and NOESY in H_2O (Fig. 2 *B*), all at 10°C. Only three kinds of amino acid resonances were observed, corresponding to Thr, and two Ala residues. This is consistent with a repeated unit of $(AAT)_n$. All of the protons could be assigned to residue type. In addition, all of the sugar protons could be assigned to β-Gal or GalNAc (Table 1). Only one set of resonances for the disaccharides was observed. This is again consistent with a simple repeated unit $(AAT^*)_n$. ^{13}C assignments were obtained for all protiated carbons (Table 1) using the ^{13}C-^1H HSQC experiment (Fig. 3). The improved resolution of the spectra allowed unambiguous and complete assignments of both sugar residues, unlike previously for AFGP8 where the four GalNAc residues were non-equivalent (Lane et al., 1998; Dill et al., 1992). The shifts in Table 2 revise some previous assignments of comparable fragments (Homans et al., 1985). The 1D ^{13}C and HSQC spectra (Fig. 3) showed only a single set of resonances for the (AAT*) repeating unit. All of the ^{13}C resonances were narrow compared with linewidths predicted for a 20–30-kDa globular protein, indicating the presence of significant internal mobility in the molecule. Furthermore, there is substantial variation in the ^{13}C linewidths, especially comparing the carbons atoms of the amino acid backbone and the GalNAc with the carbon atoms of β-Gal, which suggests differences in the mobility of these residues.

^1H- and ^{13}C-NMR assignments were also obtained for the pentapeptides, which showed ^1H and ^{13}C chemical shifts very close to those observed for random coil peptides (Wishart et al., 1995). No significant non-sequential NOEs were observed, indicating that there is no stable secondary structure present in these peptides.

NMR dynamics

To characterize the internal dynamics of the glycoprotein in greater detail, we have measured ^{13}C-NMR relaxation rate constants (R_1, R_2, and NOE) at two temperatures (Table 2). The large $\{^1H\}$-^{13}C-NOEs and relatively small R_2 values imply substantial motion on the sub-nanosecond time scale. The substantial variation in R_2 values is also evident in the linewidths in 1D ^{13}C spectra (Fig. 3); the linewidths of the β-Gal carbon resonances are substantially narrower than those in the NAcGal residues or the Cα of the amino acids.

The relaxation data were quantitatively analyzed with the Lipari-Szabo (1982) method to give values for τ_0, S^2, and τ_e for each C-H vector (Table 2) as described for AFGP8 (Lane et al., 1998). The R_2 values of some residues were relatively poorly determined at 10°C as the decay was so fast, leading to a relatively large residual error. However, the fast decay is consistent with the independently observed linewidths measured from 1D ^{13}C-NMR spectra (cf. Fig. 3). The three-parameter fit gave very small residuals ($<1\%$), implying that the simple model adequately accounts for the relaxation data. However, for a few sites, especially associated with the NAc-galactosamine residue, the fit was considerably poorer, and the correlation time estimated from R_1 and the NOE alone was smaller than that implied by the large value of R_2. This could be modeled as an exchange contribution (Table 2). Such an exchange contribution to relaxation has often been observed in ^{15}N relaxation of proteins, and is usually attributed to a slow conformational equilibrium (Clore et al., 1990; Szyperski et al., 1993; Marsden et al., 1998). It is notable that the exchange contribution is larger at 10°C than at 30°C, which is in accord with the linewidths at the two temperatures. This

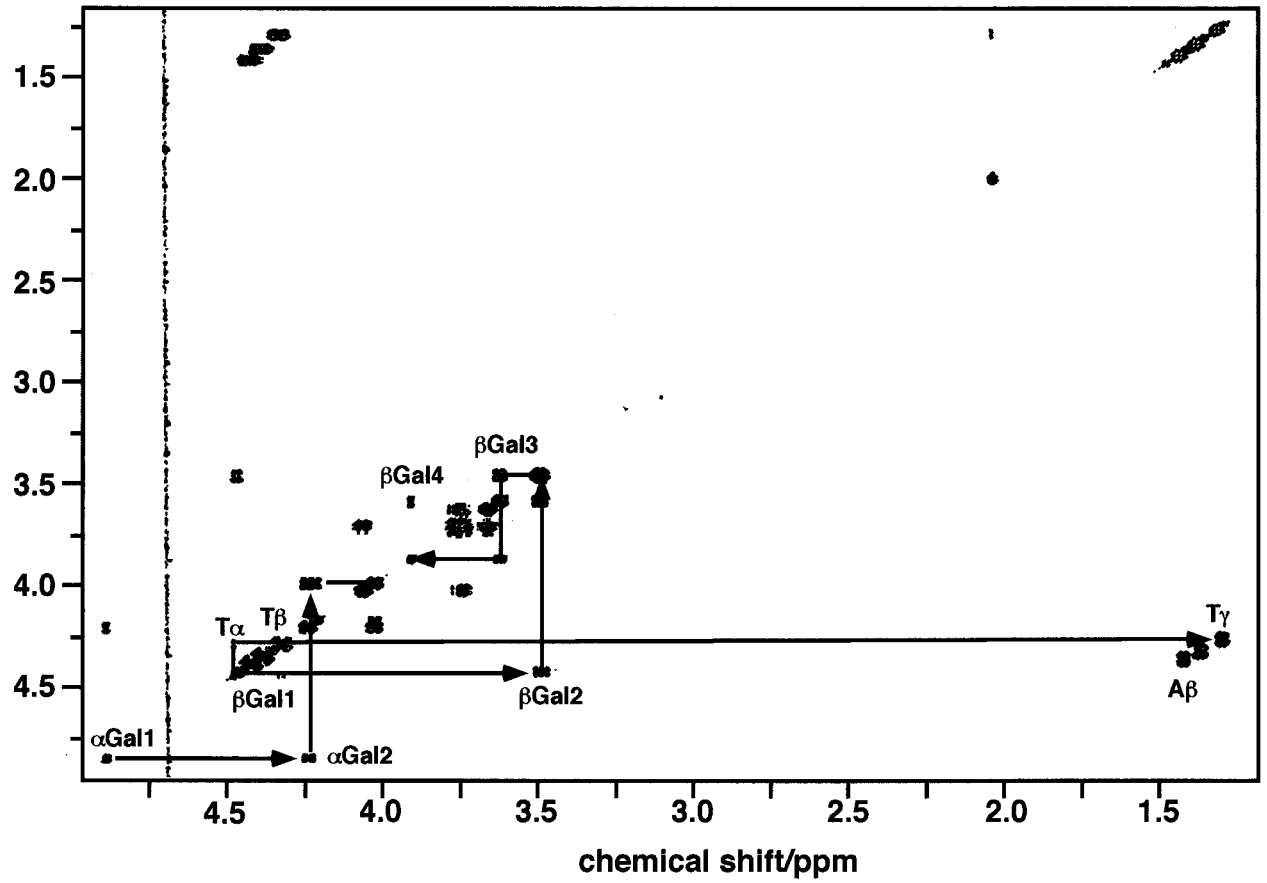

FIGURE 1 DQF-COSY spectrum of AFGP1–5 in D_2O. The spectrum was recorded at 11.75 T, 303 K with acquisition times of 0.4 s in t_2 and 0.098 s in t_1. The data table was zero-filled once in t_2 and twice in t_1, and multiplied by a shifted Gaussian function in each time dimension before Fourier transformation. The final digital resolution was 1.2 Hz per point in F2 and 2.4 Hz per point in F1. The lines show spin systems of Thr and the two Gal residues.

suggests that the exchange contribution is fast compared with the chemical shift difference, and that at lower temperatures, the system approaches the intermediate exchange regime as the rate constant decreases.

The mean value of τ_0 was 4.8 ± 0.9 ns (range = 3–6.8 ns) at 10°C and 3.5 ± 0.8 ns (range = 2.3–4.7 ns) at 30°C (Table 2). For comparison, AFGP8 gave τ_0 = 3.6 ± 1.8 ns at 5°C when analyzed in the same way using the previously reported relaxation data (Lane et al., 1998). Thus, the effective correlation time of the large AFGP1–5 protein is about the same at 30°C as that of AFGP8 at 5°C. The ratio of the site correlation time at 283 K to that at 303 K is 1.6 ± 0.3, which is comparable to the that expected from the temperature dependence of the viscosity of D_2O (Wilbur et al., 1976). As expected, the order parameters for the methyl carbons are much smaller than for the other carbons owing to free rotation of the methyl group (S^2(methyl) = 0.11). The order parameters for the C6 positions of the two sugars are intermediate in size, indicating substantial freedom of motion of the CH_2OH group. The order parameters for C–H groups are slightly larger at 10°C than at 30°C. They also can be ranked in terms of peptide backbone (Ala and Thr) and the two sugars, such that S^2(amino acid residues) > S^2(NAc-Gal) > S^2(Gal). This reflects the relative distance of the β-Gal residues from the backbone of the molecule, and shows that these sugars are highly mobile with respect to the remainder of the molecule. In addition, the Cα generally have higher order parameters than the side chains.

The range of τ_0 observed at either temperature is not consistent with a spherical rotor. However, the assumption of a rod-like structure (or other symmetric top rotor model) leads to physically implausible axial ratios; a rigid anisotropic rotor is an inappropriate model. In fact, the relatively low order parameters at the backbone sites (CαH) indicate the presence of substantial internal mobility.

The ^{13}C relaxation data show that AFGP1–5 is a rather flexible molecule, such that local segmental correlation times are comparable to those observed in the much shorter AFGP8 (Lane et al., 1998). The short effective correlation time is consistent with a persistence length of a few amino

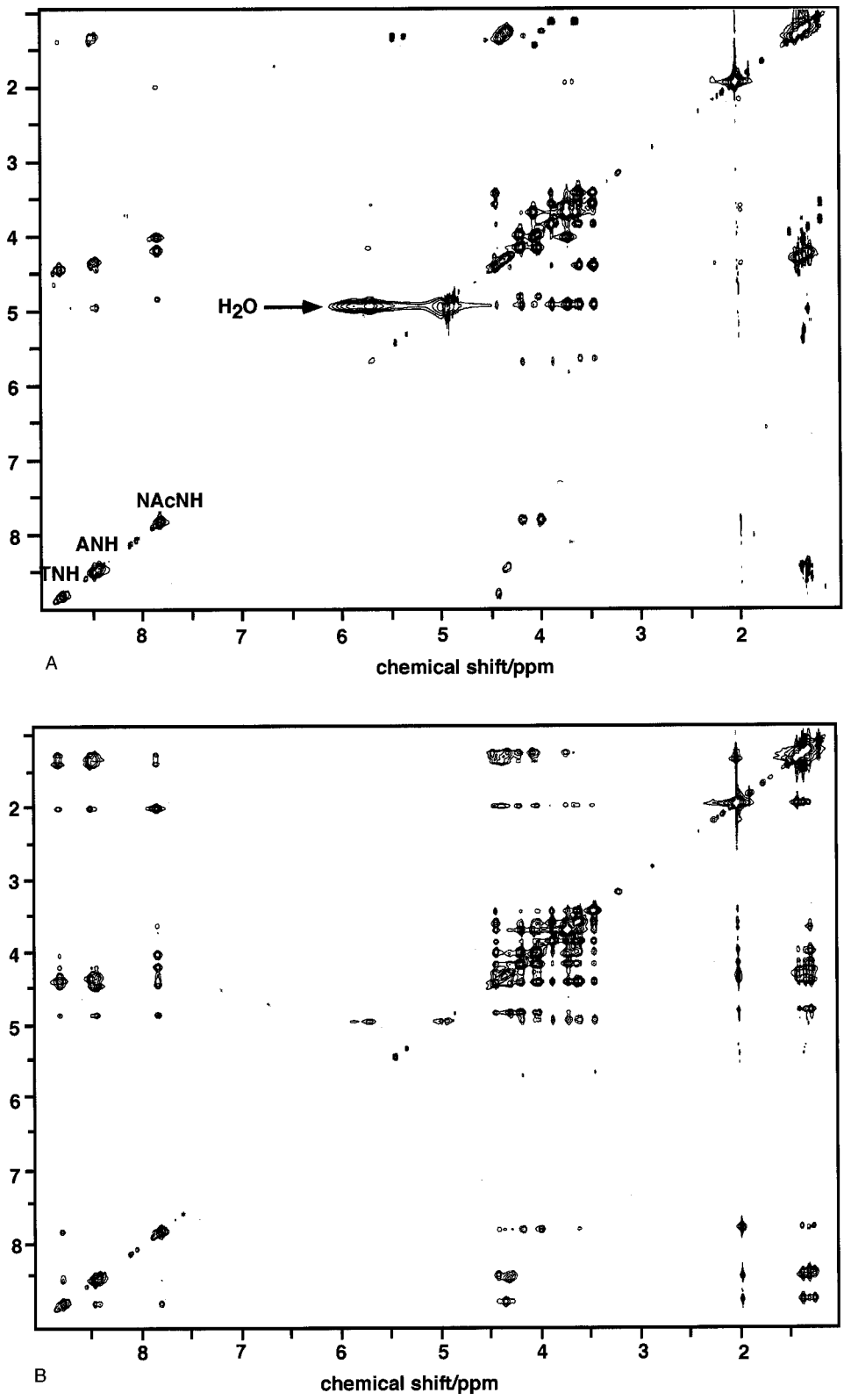

FIGURE 2 NOESY and TOCSY spectra of AFGP1–5 in H_2O. Spectra were recorded at 11.75 T and 278 K. The acquisition times were 0.41 s in t_2 and 0.102 s in t_1. Data tables were zero-filled once in t_2 and twice in t_1, and multiplied by a Gaussian function centered at $t = 0$ before Fourier transformation. The relaxation delay was 2 s. (*A*) TOCSY with a mixing time = 47 ms, $\gamma B_1 = 8.2$ kHz. (*B*) NOESY with a mixing time of 200 ms.

acid residues (Schwalbe et al., 1997). However, the presence of a disaccharide every third residue should make the persistence length comparable to the length of the repeating unit, namely AAT*. In addition, the sugar residues (especially β-Gal) must be fully exposed to solvent, and essentially unconstrained. The simple picture of the dynamics of the glycoprotein is that of essentially a random coil showing large-scale segmental flexibility on the sub and nanosecond

TABLE 1 NMR assignments of AFGP1-5

Proton	^{1}H	^{13}C
A1NH	8.53	—
A1α	4.42	51.9
A1Me	1.42	19.5
A2NH	8.59	—
A2α	4.38	51.5
A2Me	1.37	20.0
TNH	8.90	—
Tα	4.49	60.0
Tβ	4.33	78.8
TMe	1.29	20.5
NHAc	7.9	—
NHAcMe	2.03	25.0

	^{1}H (^{13}C)					
Sugar	1	2	3	4	5	6
β-Gal	4.48 (107.5)	3.49 (73.5)	3.62 (75.2)	3.91 (71.4)	3.66 (77.6)	3.75 (63.9)
α-Gal-NAc	4.89 (101.5)	4.24 (51)	4.03 (80.2)	4.21 (71.5)	4.08 (73.7)	3.74 (64.0)

Chemical shifts are quoted for 30°C except for NH, which are for 10°C. The sequence is $(A1A2T3^*)_n$.

time scale (Bush and Feeney, 1986). The presence of only a few sequential, short-range NOEs for the amino acids is also consistent with the absence of substantial long-range order.

The value of $^3J_{\alpha\beta}$ measured or the Thr residue was 4–5 Hz, which is larger than expected for either g^+ or g^- rotamers ($^3J < 4$ Hz) and much smaller than for the *trans* rotamer ($^3J > 12$ Hz). This indicates that the population of the *trans* rotamer is relatively small. This coupling constant is similar to that observed in the peptide NAcAATAA.

Translational diffusion

The translational diffusion coefficient of AFGP1–5 was measured in D_2O at 10°C and 30°C, under the same conditions as the ^{13}C-NMR relaxation measurements. Fig. 4 shows the decay data at the two temperatures, fitted to a single Gaussian. A slight improvement in the fit was obtained with a sum of two Gaussians, but the amplitude of the second Gaussian was relatively small, and the diffusion coefficient was not well determined. It is possible that this second component corresponds to some of the minor species present in the AFGP1–5 mixture. The translational diffusion coefficients were determined as $5.1 \cdot 10^{-7}$ cm^2 s^{-1} at 30°C and $2.71 \cdot 10^{-7}$ cm^2 s^{-1} at 10°C. Normalization to water at 20°C gives $D_{20,w} = 4.8$ and 4.6 10^{-7} cm^2 s^{-1}, respectively. Thus, the diffusion coefficient follows the expected dependence on solvent temperature (and viscosity). This normalized value is similar to that previously reported for fraction 4 (Ahmed et al., 1975) and for fractions 1–5 determined by quasi-elastic light scattering (Wilson and deVries, 1994). The normalized value is ~60% of that determined for the globular protein carbonic anhydrase ($M_r = 30$ kDa). As diffusion coefficients scale as $M_r^{-1/3}$, this implies a particle that generates much more friction than a globular protein, and is consistent with an extended molecule that is fully solvated. Thus, the rotational and translational diffusion data indicate an unstructured, segmentally flexible molecule.

Interactions with water

At 5°C, two resonances at 5.75 and 5.9 ppm were observed in H_2O (Fig. 5 *A*) that do not appear in spectra recorded in D_2O. Thus, these protons must be readily exchangeable with solvent hydrogens, such as NH or OH. As all of the NH have been accounted for at much lower field, these resonances are likely to arise from carbohydrate hydroxyls (Poppe and van Halbeek, 1994; Leroy et al., 1985). One of these resonances appears as a doublet. This shows crosspeaks in both TOCSY (Fig. 2 *A*) and ROESY (Fig. 5 *B*) with the H2/3 of β-Gal, whereas the broader peak shows an interaction with the C6 of β-Gal and/or α-GalNAc. These resonances belong to sugar hydroxyls, and plausibly are those on the C2/C3 of β-Gal and the C6, respectively.

The ROESY spectrum (and NOESY) also shows crosspeaks between the water resonance, and protons in the two sugar moieties. Most of the sugar carbons (not the anomeric) have a hydroxyl group. As only two hydroxyl protons have been accounted for by the downfield-shifted resonances, it is probable that the remaining hydroxyl protons are coincident with the water resonance. These additional crosspeaks therefore represent ROEs between hydroxyl protons and the proton attached to the same carbon atom. These ROEs are likely also to be mediated by exchange with water protons (Gyi et al., 1998).

FTIR spectroscopy of AFGP1–5 and AFGP8

FTIR provides information about conformation of the peptide backbone via the frequency of the amide I band. The IR

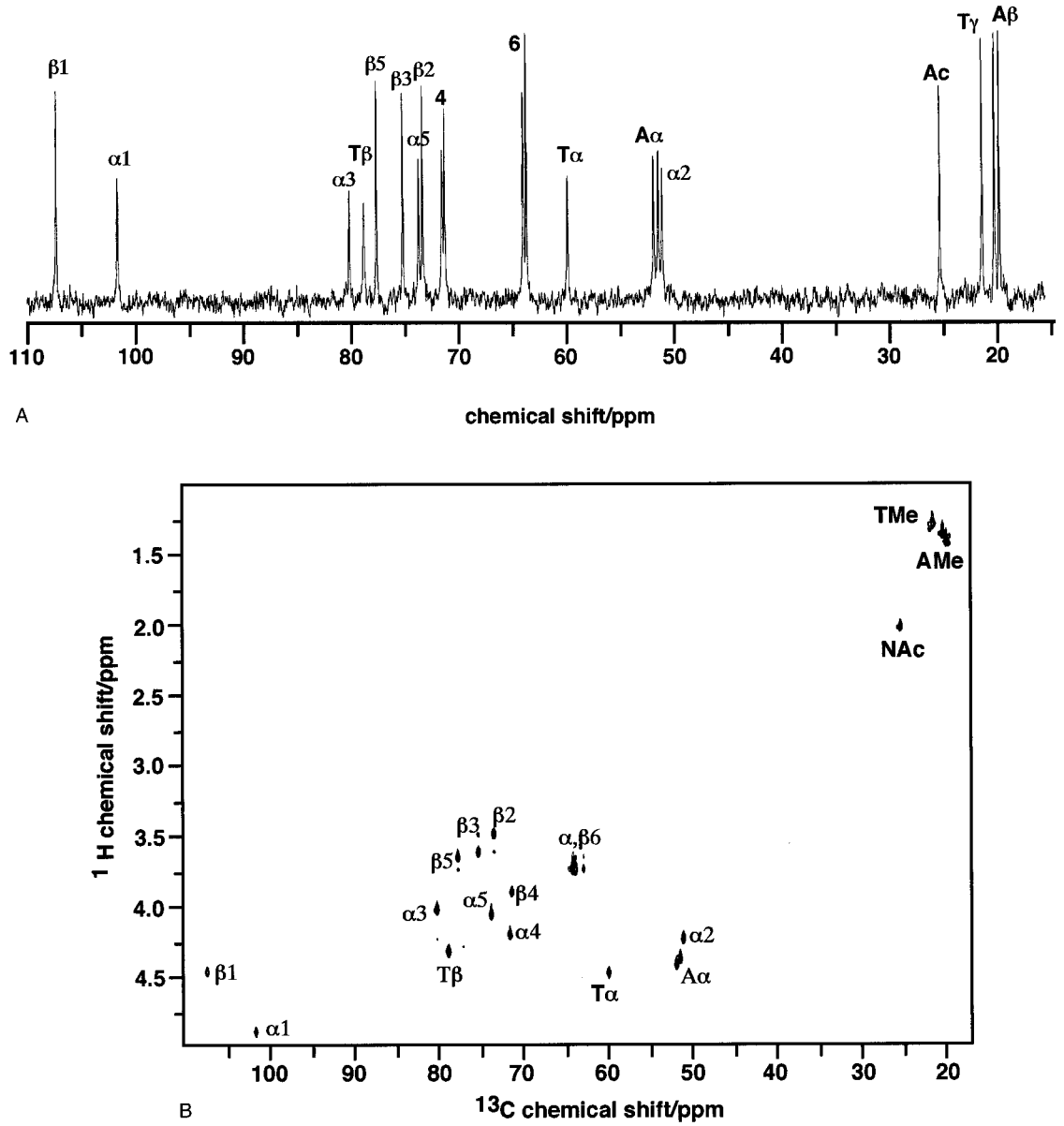

FIGURE 3 ^{13}C-NMR spectra of AFGP1–5. (*A*) 1D ^{13}C spectrum recorded at 303 K and 9.4 T with Waltz decoupling. (*B*) HSQC spectrum. The spectrum was recorded at 14.1 T and 30°C with acquisition times of 0.1 s in t_2 and 0.057 s in t_1. Data tables were zero-filled twice in t_2 and twice in t_1, and multiplied by a Gaussian function centered at $t = 0$ before Fourier transformation, giving final digital resolutions of 2.5 Hz/point in F2 and 4.39 Hz/point in F1.

spectra of AFGP8 and AFGP1–5 are quite different (Fig. 6); the distribution of resolvable bands is more even across the frequency range for AFGP8 than for AFGP1–5. Independent of the precise assignment of the observed IR bands, AFGP1–5 is significantly different from AFGP8. The frequencies and relative peak areas are given in Table 3. The different C═O stretch frequencies have been associated with different types of secondary structure (Dong et al., 1990, 1992, 1994; Pestrelski et al. 1991), which may mean that the amide I frequency reflects the local ø, ψ angles, either directly through hybridization, by affecting hydrogen bonding to the solvent, or indirect local electrostatic influences of the orientation of the amino acid with respect to the plane of the peptide bond. The precise assignment of bands to secondary structure types, however, remains controversial (Surewicz et al., 1993).

In AFGP8 there are only 13 peptide bonds, including two from proline. It is rather unlikely that both helical and extended strand conformations could be simultaneously present in such a short peptide. The alternative would be that at any one moment a substantial fraction of molecules would be essentially all helix, and a similar fraction of molecules would be in an extended conformation. Similarly, for AFGP1–5, the IR data indicate substantial amounts of

TABLE 2 ^{13}C relaxation of AFGP1-5

	R_1 (s^{-1})		R_2 (s^{-1})		NOE (s^{-1})		τ_0 (ns)		S^2 (s^{-1})		R_x* (s^{-1})	
Carbon	283†	303†	283†	303†	283†	303†	283†	303†	283†	303†	283†	303†
β-Gal-1	3.25	3.47	17.3	7.83	1.58	1.71	4.9	2.7	0.73	0.47		
β-Gal-2	3.4	3.35	18.0	7.91	1.62	1.80	5.1	2.9	0.73	0.45		
β-Gal-3	3.86	3.44	16.3	7.46	1.59	1.64	4.5	2.5	0.73	0.49		
β-Gal-4	3.32	3.54	25.3	12.5	1.53	1.78	4.5	4.1	0.73	0.57		
β-Gal-5	3.62	3.50	16.1	7.23	1.60	1.80	4.5	2.6	0.71	0.43		
β-Gal-6	3.08	2.32	9.85	4.32	1.90	2.34	4.0	3.4	0.45	0.16		
α-Gal-1	2.90	4.03	32.5	13.8	1.50	1.35	6.2	3.3	0.82	0.82	9.5	
α-Gal-2	3.88	4.32	20.5	13.8	1.42	1.61	5.2	2.8	0.84	0.63		3
α-Gal-3	2.57	4.25	35.0	13.6	1.50	1.57	6.8	3.6	0.82	0.71	9.9	
α-Gal-4	3.21	3.71	42.0	16.6	1.40	1.62	5.2	4.7	0.86	0.71	21	
α-Gal-5	3.19	3.91	33.3	15.7	1.46	1.70	4.9	3.4	0.80	0.59	14.8	4.5
α-Gal-6	3.34	3.04	17.9	6.35	1.86	2.09	6.2	3.0	0.59	0.29	13	
N-Ac	0.71	0.53	2.16	1.20	1.26	1.46	3.0	3.5	0.14	0.18		
Thr-α	3.55	4.46	30.8	14.8	1.37	1.46	4.2	3.6	0.84	0.8		
Thr-β	2.56	4.49	52.0	18.1	1.34	1.60	5.3	2.8	0.76	0.65	33.6	7.4
Thr-Me	1.2	0.89	3.06	1.54	2.29	2.26	4.4	3.6	0.14	0.06		
Ala-1α	2.85	3.95	24.8	12.8	1.32	1.81	5.6	4.1	0.88	0.57	13	
Ala-1Me	1.2	0.87	3.13	1.53	2.34	2.18	4.2	2.4	0.12	0.08		
Ala-2α	3.45	4.35	28.7	14.6	1.37	1.59	4.0	2.8	0.8	0.65	14.1	3.9
Ala-2Me	1.3	1.0	3.76	1.85	2.3	2.49	3.9	2.4	0.12	0.08		

Relaxation rate constants were determined at 9.4 T as described in the Methods. The values of R_1 and R_2 have been normalized to the number of directly bonded protons.

*R_x is the exchange rate constant estimated as described in the text; no entry implies a value of <1 s^{-1}.

†T/K.

α-helix and β-sheet, yet the NMR data show that such structures must be present in low amounts.

CD and NMR experiments have indicated the presence of polyproline type II helix in AFGP8 (Bush et al., 1984; Lane et al., 1998). With FTIR analysis, a pure polyproline sample (50 mg/ml) has over 80% of the amide region centered on 1618 ± 2 cm^{-1} (Hays, 1998). Most FTIR users consider this wavenumber to be outside of the amide I region, and it is usually defined as the vibrational frequency of side chains (Chirgadze et al., 1975). However, Ala, Thr, and Pro do not absorb in this region. This region may also include intermolecular β-sheets due to protein aggregation (for review see Dong et al., 1995). However, the IR spectrum of polyproline lacks the 1685 cm^{-1} peak that is also present in protein aggregates. The NMR spectra also show no evidence of significant aggregation. In the AFGP8 spectra, a

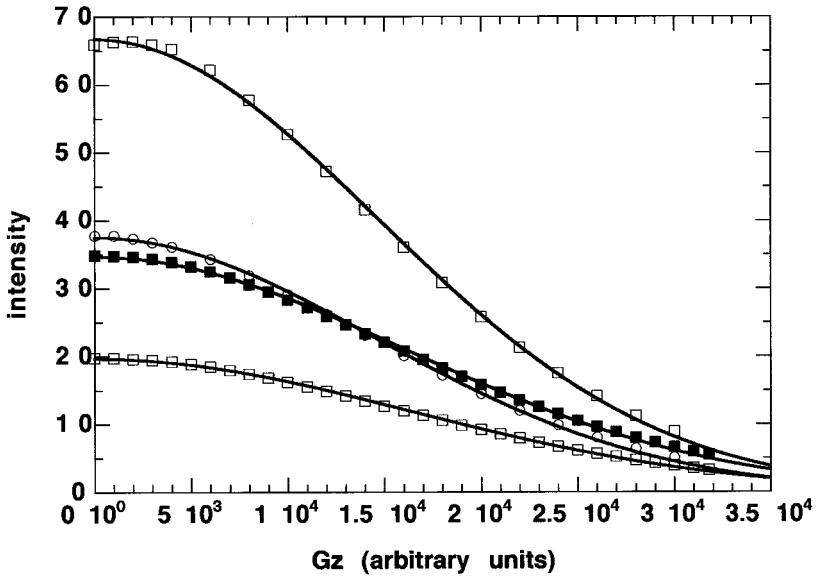

FIGURE 4 Diffusion of AFGP1–5. 1D spectra were recorded at 303 K and 283 K in D_2O at 14.1 T as a function of the *z*-gradient strength. Intensity versus gradient strength for the regions 4.51–3.15 ppm (□, ■) and 1.56–0.95 (○, ●) ppm at 30°C and 10°C.

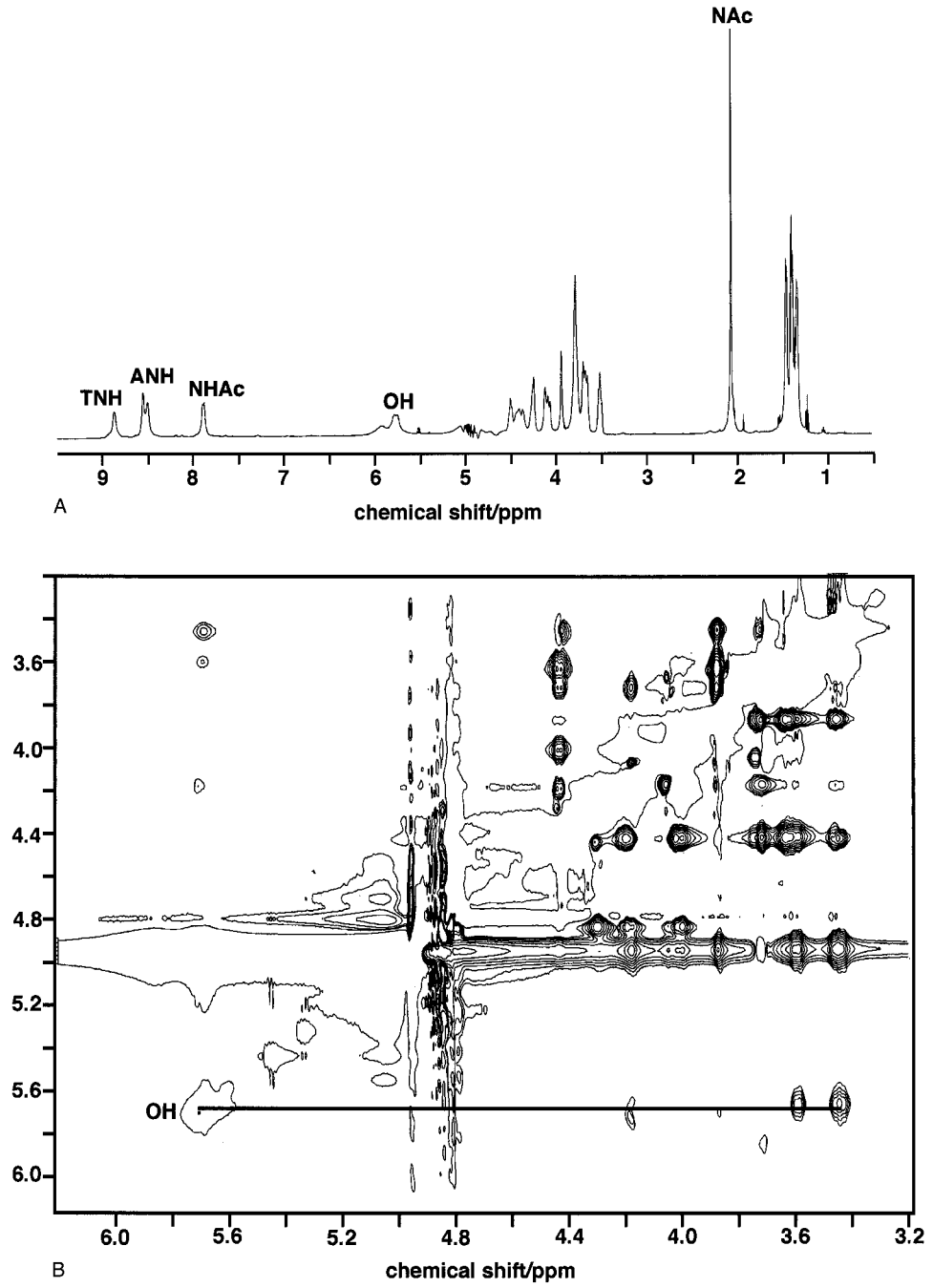

FIGURE 5 Hydroxyl protons in AFGP1–5. Spectra were recorded at 11.75 T and 278 K. (*A*) The 1D spectrum was recorded with an acquisition time of 1.5 s and a recycle time of 4 s. (*B*) The ROESY spectrum was recorded with a continuous wave spin lock ($\gamma B_1 = 4.3$ kHz) centered at the water frequency with a mixing time of 40 ms. The acquisition times were 0.41 s in t_2 and 0.102 s in t_1. The single contour is positive (diagonal and exchange peaks), the multiple contours are negative (ROEs).

substantial peak was observed at 1620 cm^{-1}, whereas for AFGP1–5, there was a much lower intensity at this wavenumber (Table 3). However, it is not obvious that the IR frequency of the polyPro II conformation will be the same for non-Pro residues. The band at 1645–1650 cm^{-1} has been assigned to an unordered conformation (Table 3). However, it has been suggested, based on ultraviolet circular dichroism and vibrational circular dichroism, that this frequency corresponds at least in part to the polyPro II conformation (Woody, 1992). This suggests that the two classes of antifreeze glycoproteins differ mainly in the distribution of possible conformers, which we expect to reflect the influence of the Pro residues on the local conformation in AFGP8 (Lane et al., 1998). Because of the possible distortions of band areas introduced by taking the second derivative, and because the absorption coefficients for the different conformers are not known to be the same, the actual populations cannot be accurately calculated from the IR data.

NMR spectra of the two pentapeptides NAcAATAA and NAcAAPAA show dynamically unstructured peptides (data not shown). The FTIR spectra of the same peptides show

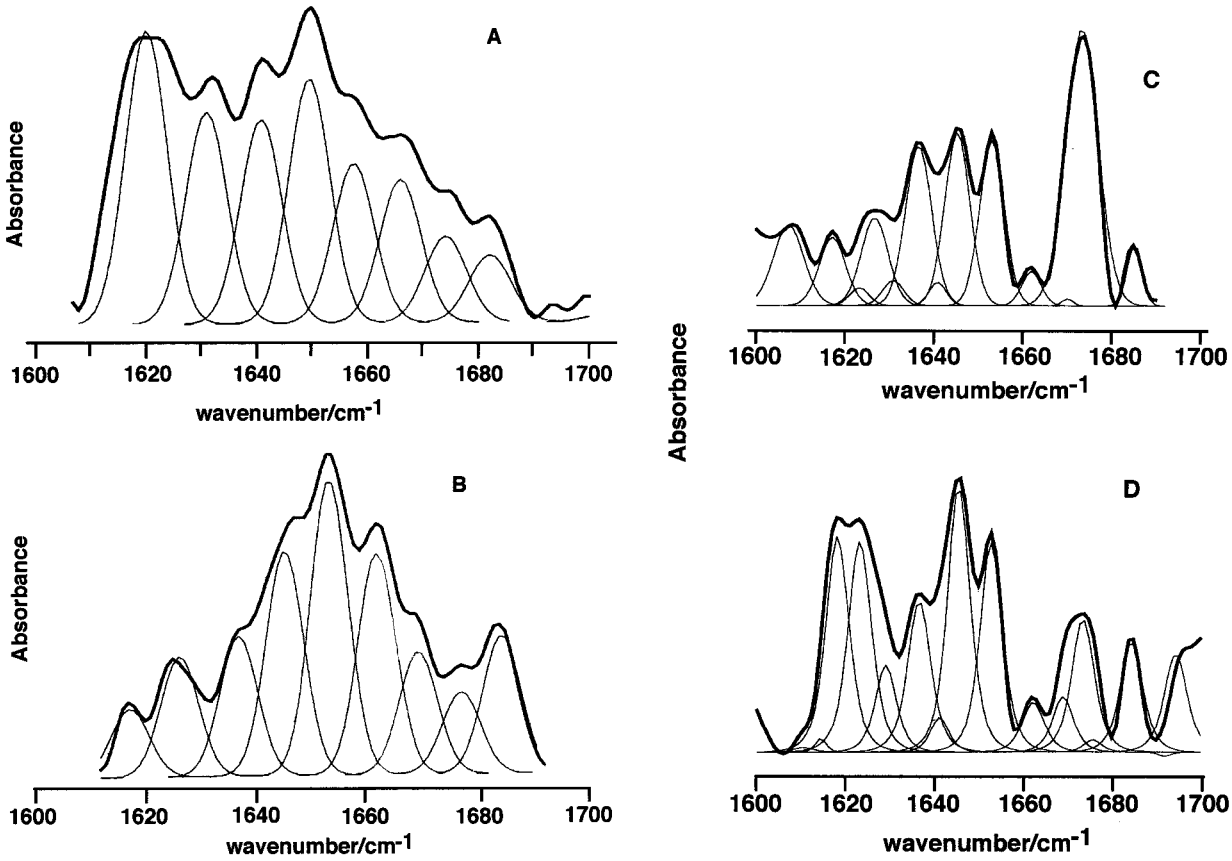

FIGURE 6 FTIR spectra of AFGP1–5 and AFGP8 and peptides. Spectra were recorded as described in the Experimental section. They are displayed as second derivatives, with Gaussian band fits. (*A*) AFGP8; (*B*) AFGP1–5; (*C*) NAcAATAA; (*D*) NAcAAPAA.

numerous bands ranging from 1610 to 1680 cm^{-1}, analogously to those observed in the AFGPs, and the pattern of observed bands is significantly different for the Pro- and Thr-containing peptides (Fig. 6). This clearly shows that these short peptides populate the allowed regions of Ramachandran space, and interconvert slowly compared with the difference between their respective vibrational frequencies. The similarity to the FTIR spectra of the AFGPs indicates that the carbohydrate is not responsible for the slow interconversion rates between the various conformations.

TABLE 3 Amide I bands in AFGP8 and AFGP1-5 and apparent secondary structures

Wavenumber/cm^{-1}		Relative area (%)		Secondary structure type
AFGP8	AFGP1-5	AFGP8	AFGP1-5	
1619 ± 1	1619 ± 2	19 ± 2	9 ± 3	Polyproline*
1630 ± 1	1630 ± 2	14 ± 6	15 ± 3	Extended†
1639 ± 2	1637	13 ± 4	10	Extended†
	1645 ± 3		16 ± 3	Unordered†
1649 ± 1		22 ± 5		Unordered†
1658 ± 1	1655 ± 1	10 ± 1	23 ± 1	α-Helix†
	1661		19 ± 3	3_{10} Helix†
1667 ± 1	1667 ± 2	14 ± 4	15 ± 4	Turn†
1676 ± 2	1677	6 ± 1	6	Turn†
1684 ± 2	1682 ± 2	4 ± 1	5 ± 1	Turn†

Spectra were recorded and analyzed as described in the Methods. Frequencies and areas are the given as the mean and standard deviation ($n = 3$).
*Assignment from Hays (1998).
†Assignments from Dong et al. (1990) and Pestrelski et al. (1991).

MD calculations

From molecular dynamics simulations in water it is possible to assess the mobility of protein backbone atoms on the sub-nanosecond times scale and compare them with experimental NMR data. Typically, for folded proteins, the order parameters of NH and CαH vectors are in the range 0.8–0.9 in defined secondary structure elements, and the local correlation times are usually all very similar (Clore et al., 1990; Kördel et al., 1992; Lüginbuhl et al., 1997; Nicholson et al., 1996). Unstructured portions of the protein, especially at chain termini, generally show a decreased local correlation time and lower order parameters (van Heijenoort et al., 1998; Alexandrovich et al., 1999). These general results are reproduced by MD simulations (J. O. Trent, S. J. Smerdon, and A. N. Lane, unpublished data). Preliminary calculations in both water (400 ps) and in vacuo (1–5 ns) show that

although the backbone torsions ø and ψ oscillate around mean values with an rmsd of ~30°, transitions between different regions of Ramachandran space are comparatively rare (~1–3 times every nanosecond), and not obviously correlated between neighboring dipeptide units. This is slow on the infrared time scale, such that separate bands for extended, turn, and helix would give rise to separate bands. It is, however, fast on the time scale of NMR coupling constants and chemical shifts, which would therefore not give rise to separate lines, and coupling constants should reflect averaged values. The high-frequency fluctuations of Cα and Cβ are fast on the NMR relaxation time scale, and would be expected to give NMR order parameters substantially less than unity.

DISCUSSION

According to the NMR data, AFGP8 has no long-range order, but displays significant local order (Lane et al., 1998). In contrast, AFGP1–5 is a dynamically disordered molecule that shows neither significant long-range nor short-range order on a time scale from 100 ps to milliseconds. At face value the IR data indicate that although the AFGP fractions are different at the backbone level, they both contain substantial amounts of secondary structure elements. The IR results can be rationalized with the NMR data by considering the time scales probed by the two methods. The spread of wavenumbers for different regions of Ramachandran space is ~60 cm^{-1} centered at 1650 cm^{-1} (Table 1), which is equivalent to a characteristic time scale of $>10^{12}$ s^{-1}. Interconversion between conformational states on a slower time scale leads to individual peaks corresponding to all conformations that are present in an ensemble. It has recently been shown by Raman spectroscopy that unordered polypeptides show several vibration frequencies, which was interpreted in terms of an ensemble of conformation states (Sane et al., 1999). This is supported by molecular dynamics simulations of Ala-8 peptides in water, which showed substantial high-frequency fluctuations (a few picoseconds) about ø and ψ, and rarer transitions between the α_R, $\alpha_L\beta$, and polyPro II regions of Ramachandran space (Sreerama and Woody, 1999). In contrast, the same interconversion rates would be fast on the NMR chemical shift time scale (~10^3 s^{-1}), and therefore the NMR resonances appear at a single averaged frequency. This is similar to the observed behavior of short hormonal peptides in solution (Feeney, 1977). In addition to the relatively slow rotational motions of groups of residues (~5–8) on the 3–7-ns time scale, there are higher-frequency motions (tens to hundreds of picoseconds) of substantial amplitudes, as shown by the NMR order parameters. Values of S^2 ~0.5 are roughly equivalent to angular fluctuations of ~35–40° on the sub-nanosecond time scale. Hence, there are large amplitude motions of the Cα-H vectors that require substantial changes in the ø, ψ angles, presumably within the allowed regions of Ramachandran space. There is an ensemble of conformations interconverting rapidly on the NMR time scale, and slowly on the IR time scale. Hence, in IR even a random coil will show different bands corresponding to an ensemble of molecules that occupy different regions of Ramachandran space, whereas in NMR there will be a single resonance for each proton or carbon atom. The simplest interpretation of the IR and NMR data together is that the molecules are flexible, such that each dipeptide unit occupies several regions of Ramachandran space for various amounts of time. Because ø in proline is essentially fixed by the covalent structure, proline-containing dipeptides have fewer degrees of freedom than other dipeptides. This can be expected to restrict the conformational space accessible to the proline-containing AFGP8 compared with the proline-free AFGP1–5. For AFGP1–5, a wide variety of backbone torsions are significantly populated, giving rise to numerous bands in the IR spectrum, whereas in AFGP8 the degree of Ramachandran space that is accessed is lower than in the proline-free AFGP1–5, giving rise to a narrower distribution of IR bands having significant intensity (>15–20%). This is supported by the NMR and FTIR spectra of the pentapeptides. These findings have implications for the analysis of secondary structures of proteins by IR, as the so-called unordered frequency does not account for all of the non-secondary structure peptides. The helical, turn, and extended segments can be overestimated, which is likely to be more of a problem in partially folded proteins. Even in denatured or unstructured proteins such as casein, the observation of a very broad IR band (Byler and Susi, 1986) does not necessarily imply a single conformation, but rather an unresolved envelope of conformers.

In conclusion, the combination of NMR, IR, and MD is a powerful means of obtaining detailed information about the conformational properties and dynamics of macromolecular systems. It is becoming increasingly clear that biological activity is not restricted to compact semi-rigid proteins. However, many of the methods of analysis and the philosophical underpinnings of protein action are couched in terms of single conformations or simple conformational changes. The activity of highly flexible molecules that may or may not fold into a unique conformation on binding to a "receptor" poses a challenge for conformational analysis. Not least is the need to describe ensemble properties and the dynamic of interconversion within the ensemble. It is usually not possible to obtain sufficient experimental data to determine the conformations present in such an ensemble. However, the combination of experimental methods and molecular dynamics may be able to provide a description of the general conformational properties and the extent to which conformational space is populated, albeit in a non-unique manner.

We thank Dr. T. A. Frenkiel for valuable discussions.

This work was supported by the Medical Research Council of the UK and by National Institutes of Health Grant R01HL57810-01.

REFERENCES

Ahmed, A. L., R. E. Feeney, D. T. Osuga, and Y. Yeh. 1975. Antifreeze glycoproteins from an Antarctic fish. Quasi-elastic light scattering studies of the hydrodynamic conformations of antifreeze glycoproteins. *J. Biol. Chem.* 250:3344–3349.

Alexandrovich, A., G. F. Moolenaar, N. Goosen, M. R. Sanderson, and A. N. Lane. 1999. Solution conformation and stability of the dimerization domain of uvrB from *E. coli. FEBS Lett.* 451:181–185.

Allison, S. D., A. Dong, and J. F. Carpenter. 1996. Counteracting effects of thiocyanate and sucrose on chymotrypsinogen secondary structure and aggregation during freezing, drying, and rehydration. *Biophys. J.* 71: 2022–2032.

Bax, A., R. H. Griffey, and B. L. Hawkins. 1983. Correlation of proton and nitrogen-15 chemical shifts by multiple quantum NMR. *J. Magn. Reson.* 55:301–315.

Burcham, T. S., D. T. Osuga, Y. Yeh, and R. E. Feeney. 1986. A kinetic description of antifreeze glycoprotein activity. *J. Biol. Chem.* 261: 6390–6397.

Bush, C. A., and R. E. Feeney. 1986. Conformation of the glycotripeptide repeating unit of antifreeze glycoprotein of polar fish as determined from the fully assigned protein n.m.r. spectrum. *Int. J. Pept. Prot. Res.* 28:386–397.

Bush, C. A., S. Ralapati, G. Matson, R. B. Yamasaki, D. T. Osuga, Y. Yeh, and R. E. Feeney. 1984. Conformation of the antifreeze glycoprotein of polar fish. *Arch. Biochem. Biophys.* 232:624–631.

Byler, D. M., and H. Susi. 1986. Examination of the secondary structure of proteins by deconvolved FTIR spectra *Biopolymers*. 25:469–487.

Chirgadze, Y. N., O. V. Federov, and N. P. Trushina. 1975. Estimation of amino acid residue side-chain absorption in the infrared spectra of protein solutions in heavy water. *Biopolymers.* 14:679–694.

Clore, G. M., P. C. Driscoll, P. T. Wingfield, and A. M. Gronenborn. 1990. Analysis of the backbone dynamics of interleukin-1 beta using two-dimensional inverse detected heteronuclear ^{15}N-^{1}H-NMR spectroscopy. *Biochemistry.* 29:7387–7401.

Davies, P. L., and B. D. Sykes. 1997. Antifreeze proteins. *Curr. Opin. Struct. Biol.* 7:828–834.

DeVries, A. L., S. K. Komatsu, and R. E. Feeney. 1970. Chemical and physical properties of freezing point-depressing glycoproteins from Antarctic fishes *J. Biol. Chem.* 245:2901–2908.

Dill, K., L. Huan, D. W. Bearden, and R. E. Feeney. 1992. Structural studies of Antarctic fish antifreeze glycoproteins by one- and two-dimensional NMR spectroscopy *J. Carb. Res.* 11:499–517.

Dong, A., W. S. Caughey, and T. W. Du Clos. 1994. Effects of calcium, magnesium, and phosphorylcholine on secondary structures of human C-reactive protein and serum amyloid P component observed by infrared spectroscopy. *J. Biol. Chem.* 269:6414–6430.

Dong, A., P. Huang, and W. S. Caughey. 1990. Protein secondary structures in water from second-derivative amide I infrared spectra. *Biochemistry.* 29:3303–3308.

Dong, A., P. Huang, and W. S. Caughey. 1992. Redox-dependent changes in β-extended chain and turn structures of cytochrome *c* in water solution determined by second-derivative amide I infrared spectra. *Biochemistry.* 31:182–189.

Dong, A., S. J. Pestrelski, S. D. Allison, and J. F. Carpenter. 1995. Infrared spectroscopic studies of lyophilization- and temperature-induced protein aggregation. *J. Pharm. Sci.* 84:415–424.

Feeney, J. 1977. The conformation of hormonal peptides in solution. *In* Drug Action at the Molecular Level. G. C. K. Roberts, editor. Macmillan Press, New York. 55–71.

Feeney, R. E. 1988. Inhibition and promotion of freezing: fish antifreeze proteins and ice-nucleating proteins. *Comm. Agric. Food Chem.* 1:147–181.

Forster, M. F. 1989. Fast repetition spin-echo method for measuring spin-spin relaxation-times *J. Magn. Reson.* 84:580–584.

Gibbs, S. J., and C. S. Johnson, Jr. 1991. A PFG NMR experiment for accurate diffusion and flow studies in the presence of eddy currents. *J. Magn. Reson.* 93:395–402.

Gupta, R. K., J. A. Ferretti, E. D. Becker, and G. A. Weiss. 1980. A modified fast inversion-recovery technique for spin-lattice relaxation measurements. *J. Magn. Reson.* 38:447–452.

Gyi, J. I., A. N. Lane, G. L. Conn, and T. Brown. 1998. Identification and hydration of C2′-OH in RNA and RNA · DNA hybrids by NMR. *Nucleic Acids Res.* 26:3104–3110.

Harding, M. M., L. G. Ward, and A. D. J. Haymet. 1999. Type I 'antifreeze' proteins. *Eur. J. Biochem.* 264:653–665.

Haymet, A. D. J., L. G. Ward, and M. M. Harding. 1999. Winter flounder "antifreeze" proteins: synthesis and ice growth inhibition of analogs that probe the relative importance of hydrophobic and hydrogen-bonding interactions. *J. Am. Chem. Soc.* 121:941–948.

Hays, L. M. 1998. Antifreeze glycoproteins from Antartic fish: their structure and function in regards to lipid thermotropic phase transitions. Ph.D. Thesis, University of California, Davis.

Homans, S. W., A. L. DeVries, and S. B. Parker. 1985. Solution structure of antifreeze glycopeptides. *FEBS Lett.* 183:133–137.

Kördel, J., N. J. Skelton, M. Akke, A. G. Palmer II, and W. J. Chazin. 1992. Backbone dynamics of calcium-loaded calbindin D9k studied by two-dimensional proton-detected ^{15}N-NMR spectroscopy. *Biochemistry.* 31: 4856–4866.

Lane, A. N., L. M. Hays, R. E. Feeney, L. M. Crowe, and J. H. Crowe. 1998. Conformational and dynamic properties of a 14 residue antifreeze glycopeptide from Antarctic cod. *Protein Sci.* 7:1555–1563.

Leroy, J-L., D. Broseta, and M. Gueron. 1985. Proton exchange and base-pair kinetics of poly(rA).poly(rU) and poly(rI).poly(rC). *J. Mol. Biol.* 184:165–178.

Lipari, A., and G. Szabo. 1982. Model-free approach to the interpretation of nuclear magnetic resonance relaxation in macromolecules. 1. Theory and range of validity. *J. Am. Chem. Soc.* 104:4546–4559.

Luginbühl, P., K. V. Pervushin, H. Iwai, and K. Wüthrich. 1997. Anisotropic molecular rotational diffusion in ^{15}N spin relaxation studies of protein mobility. *Biochemistry.* 36:7305–7312.

McIntosh, P. G., F. A. Taylor, T. A. Frenkiel, S. J. Snerdon, and A. N. Lane. 2000. The influence of DNA-binding on the backbone dynamics of the yeast cell-cycle protein Mbpl. *J. Biomol. NMR*. 16:183–196.

Marsden, I., C. Jin, and X. Liao. 1998. Structural changes in the region directly adjacent to the DNA-binding helix highlight a possible mechanism to explain the observed changes in the sequence-specific binding of winged helix proteins. *J. Mol. Biol.* 278:293–299.

Nicholson, L. K., L. E. Kay, and D. A. Torchia. 1996. NMR Spectroscopy and its Application to Biomedical Research. S. S. Sarkar, editor. Elsevier, Amsterdam. Chap. 5.

Pestrelski, S. J., D. M. Byler, and M. N. Liebman. 1991. Comparison of various molecular forms of bovine trypsin: correlation of infrared spectra with x-ray crystal structures. *Biochemistry.* 30:133–143.

Piotto, M., V. Saudek. and V. Sklenar. 1992. Gradient-tailored excitation for single-quantum NMR spectroscopy of aqueous solutions *J. Biomol. Struct.* 2:661–665.

Poppe, L., and H. van Halbeek. 1994. NMR spectroscopy of hydroxyl protons in supercooled carbohydrates. *Nat. Struct. Biol.* 1:215–216.

Sane, S. U., S. M. Cramer, and T. M. Przybycien. 1999. A holistic approach to protein secondary structure characterization using amide I band Raman spectroscopy. *Anal. Biochem.* 269:255–272.

Schurr, J. M., H. P. Babcock, and B. S. Fujimoto. 1994. A test of the model-free formulas. Effects of anisotropic rotational diffusion and dimerization. *J. Magn. Reson.* 105B:211–224.

Schwalbe, H., K. M. Fiebig, M. Buck, J. A. Jones, S. B. Grimshaw, A. Spencer, S. J. Glaser, L. J. Smith, and C. M. Dobson. 1997. Structural and dynamical properties of a denatured protein. Heteronuclear 3D NMR experiments and theoretical simulations of lysozyme in 8 M urea. *Biochemistry.* 36:8977–8991.

Sreerama, N., and R. W. Woody. 1999. Molecular dynamics simulations of polypeptide conformations in water: a comparison of, α, β, and poly(Pro)II conformations. *Proteins.* 36:400–406.

States, D. J., R. A. Haberkorn, and D. J. Ruben. 1982. A two-dimensional nuclear Overhauser experiment with pure absorption phase in four quadrants *J. Magn. Reson.* 48:286–292.

Surewicz, W. K., H. H. Mantsch, and D. Chapman. 1993. Determination of protein secondary structure by Fourier transform infrared spectroscopy: a critical assessment. *Biochemistry.* 32:389–394.

Szyperski, T., P. Luginbuhl, G. Otting, P. Güntert, and K. Wüthrich. 1993. Protein dynamics studied by rotating frame ^{15}N spin relaxation times. *J. Biomolec. NMR.* 3:151–164.

Tanner, J. E. 1970. Use of the stimulated echo in NMR diffusion studies. *J. Chem. Phys.* 52:2523–2526.

van Heijenoort, C., F. Penin, and E. Guittet. 1998. Dynamics of the DNA binding domain of the fructose repressor from the analysis of linear correlations between the ^{15}N-^{1}H bond spectral densities obtained by nuclear magnetic resonance spectroscopy. *Biochemistry.* 37:5060–5073.

Wilbur, D. J., T. DeFries, and J. Jonas. 1976. Diffusion in compressed liquid heavy water. *J. Chem. Phys.* 65:1783–1786.

Wilson, P. W., and A. L. deVries. 1994. Hydrodynamic diameter of fish antifreeze molecules by quasi-elastic light-scattering. *Cryo Lett.* 15: 127–130.

Wishart, D. S., C. G. Bigam, A. Holm, R. S. Hodges, and B. D. Sykes. 1995. ^{1}H, ^{13}C and ^{15}N random coil shifts of the common amino acids. I. Investigations of nearest neighbor effects. *J. Biomolec. NMR.* 5:67–81.

Woody, R. W. 1992. Circular dichroism and conformation of unordered polypeptides. *Adv. Biophys. Chem.* 2:37–79.

Yeh, Y., and R. E. Feeney. 1996. Antifreeze proteins: structures and mechanisms of function. *Chem. Rev.* 96:601–617.